Strain-induced insulator–metal transition in ferroelectric $BaTiO_3$ (001) surface: First-principles study*

Lin Yang(杨林)[1], Chang-An Wang(王长安)[1], Cong Liu(刘聪)[1], Ming-Hui Qin(秦明辉)[1], Xu-Bing Lu(陆旭兵)[1], Xing-Sen Gao(高兴森)[1], Min Zeng(曾敏)[1,†], and Jun-Ming Liu(刘俊明)[1,2]

[1] *Institute for Advanced Materials and Guangdong Provincial Key Laboratory of Quantum Engineering and Quantum Materials, South China Normal University, Guangzhou* 510006, *China*

[2] *National Laboratory of Solid State Microstructures and Collaborative Innovation Center for Advanced Microstructures, Nanjing University, Nanjing* 210093, *China*

(Received 28 October 2015; revised manuscript received 26 March 2016; published online 1 June 2016)

The electronic properties of TiO_2-terminated $BaTiO_3$ (001) surface subjected to biaxial strain have been studied using first-principles calculations based on density functional theory. The Ti ions are always inward shifted either at compressive or tension strains, while the inward shift of the Ba ions occurs only for high compressive strain, implying an enhanced electric dipole moment in the case of high compressive strain. In particular, an insulator–metal transition is predicted at a compressive biaxial strain of 0.0475. These changes present a very interesting possibility for engineering the electronic properties of ferroelectric $BaTiO_3$ (001) surface.

Keywords: first-principles, ferroelectricity, insulator–metal transition, strain-induced effect

PACS: 73.20.–r, 73.20.At, 77.55.fe, 72.20.–i **DOI:** 10.1088/1674-1056/25/7/077302

1. Introduction

Barium titanate $BaTiO_3$ (BTO) as a typical perovskite ferroelectric oxide has attracted a great deal of attention due to its interesting dielectric, piezoelectric and ferroelectric properties as a fascinating platform for exploring novel functionalities and technological potentials.[1,2] In particular, a significant advance in the film growth technology allows the thickness to reach extremely small dimensions of a few unit cells, allowing the films to be a substantial ingredient contributing to the electric properties of ultra-thin BTO films and other BTO-based heterostructures, such as multiferroic tunneling junctions in the case of combining BTO with other ferromagnetic layer.[3–12] Without doubt, the surfaces and interfaces in these ultra-thin structures often exhibit very different behaviors from their bulk counterparts. It has been demonstrated that the significantly enhanced polarization properties were observed in the ultra-thin epitaxial BTO films and asymmetric three-component BTO-based hetero-structures.[3,4,11] Furthermore, the ferroelectric field effect enhanced magnetoresistance was also found in the BTO-based hetero-structures.[5]

Besides, significant advances in the growth and characterization of ferroelectric thin films have highlighted the role of substrate-induced strain in enhancing or even modifying the functional properties of ferroelectric thin films. For example, the enhanced ferroelectric transition temperature (T_C) in $\sim$2.4-nm-thick BTO film,[3,13,14] the room-temperature ferroelectricity in $SrTiO_3$[15,16] and the phase transition in ferroelectric heterostructures.[17,18] This is in part because strong correlations between charges, spins and lattices determine the functional properties of the films, and these correlations are affected by structural distortions from substrate-induced strain effects.[10,14,19–23] Currently, the structure and properties of BTO ultra-thin films and surfaces were theoretically addressed,[19,24–27] but the focus has been on the ferroelectric behaviors. There has not been much work to study the strain-induced effect on electronic structure and transport of the surface.

In this study, we will perform the *ab initio* first-principles calculations on this topic for the TiO_2-terminated (001) surface of an ultra-thin BTO layer grown epitaxially on a rigid substrate. The BTO layer is treated as a uniformly strained lattice. Detailed investigation will be carried out on the electronic structure and charge distribution on the surface layer in response to the in-plane lattice strain. Our calculation results indicate that a compressive bi-axial strain of ≥ 0.0475 can enhance the polarization displacement and induce an insulator–metal transition.

2. Calculation details

Our first-principles calculation is based on the density functional theory using the VASP package (Vienna *ab initio* simulation package[28]) in its projector augmented wave

*Project supported by the National Natural Science Foundation of China (Grant Nos. 1574091, 51272078, and 51431006), the Natural Science Foundation of Guangdong Province of China (Grant No. 2015A030313375), the Science and Technology Planning Project of Guangdong Province of China (Grant No. 2015B090927006), and the Program for International Innovation Cooperation Platform of Guangzhou City, China (Grant No. 2014J4500016).

†Corresponding author. E-mail: zengmin@scnu.edu.cn

© 2016 Chinese Physical Society and IOP Publishing Ltd

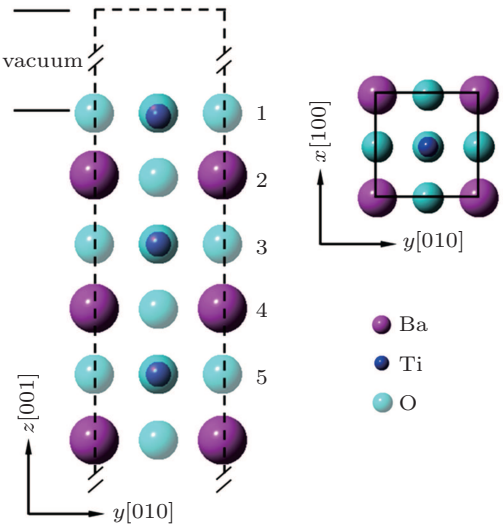


Fig. 1. (color online) Schematic arrangement in TiO_2-terminated BTO (001) surface. The solid boxes indicate the simulation cells.

(PAW) method.[29] The exchange-correlation potential was described within the generalized gradient approximation (GGA) with the Perdew–Burke–Ernzerhof (PBE) gradient correlated functional.[11] The valence electrons of Ba, Ti, and O are treated explicitly by Ba $5s^25p^66s^2$, Ti $3p^64s^23d^2$ and O $2s^22p^4$, respectively. A kinetic energy cutoff of 650 eV and a Monkhorst–Pack grid of $10\times10\times1$ k-points are employed to sample the Brillouin zone. To model a $BaTiO_3$ (001) surface, we use a 5-unit-cell (~ 2 nm) thick BTO super cell consisting of alternating TiO_2 and BaO layers in the [001] direction, as shown in Fig. 1. The atoms of the two upper united cells were allowed to relax, while all other atoms in the super cell were fixed at bulk-like. A vacuum spacer of 2 nm was used on the top to avoid undesirable periodic interaction of the surface. In our calculation only the TiO_2-terminated surface is considered as it is more stable than the BaO-terminated one.[26] Here, we define nonzero isotropic lateral strain components (ε_x, ε_y) along the x and y axis, i.e., $\varepsilon_x = \varepsilon_y \neq 0$, corresponding to the stress condition $\sigma_x = \sigma_y \neq 0$, $\sigma_z = 0$ where (σ_x, σ_y, σ_z) are the stress components. The in-plane strain ε can thus be defined as $\varepsilon = (a' - a)/a$, where a' and a are the lattice constants under strained and strain-free conditions, respectively.

For practical computation, an initial TiO_2-terminated BTO (001) surface is fully relaxed adopting experimental lattice constant $a = 4.01$ Å. Note that our relaxed lattice constant is about 3.990 Å, which is in excellent agreement with the experimental value of 3.991 Å,[23] and the relaxation structure is considered as the strain-free surface layer. Then a strained surface is established for a given strain $\varepsilon = \varepsilon_x = \varepsilon_y$. Finally, the strained surface is relaxed and the structural optimization of the equilibrium ionic positions for each case is evaluated by a damped Newton dynamics method until the Hellman–Feynman forces are less than 1.0 meV/Å.

3. Results and discussion

To quantify the process of relaxation, we use the cation–anion displacements $\delta = z_O - z_{cation}$ calculated for each BaO and TiO_2 monolayer (ML). Figure 2 shows the calculated δ as a function of ε for the BTO (001) surfaces, where three TiO_2 layers and two BaO layers are used in the calculation, as shown in Figs. 2(a) and 2(b), respectively. For the TiO_2 layers, the positive δ at the strain-free ($\varepsilon = 0$) implies that oxygen is placed above the Ti atom, indicating downward polarization $P_\downarrow$. In the top TiO_2 ML (layer 1), $\delta = 0.13$, which is in qualitative agreement with earlier calculations.[11,27] However, δ decreases rapidly toward the inner of the surfaces. The value is only 0.02 Å and near zero for the second TiO_2 ML (layer 3) and the third TiO_2 ML (layer 5), respectively. On applying the biaxial strain, the δ values decrease monotonously from compressive to tension strain, but the atom displacement almost keeps positive under these strain conditions. Once the compressive biaxial strain ε is above 0.0475, the δ values increase abruptly, which means a phase structure transition or change of properties. The reason will be discussed in the next section. For the BaO layers, the δ values are negative at ε=0, indicating an upward polarization $P_\uparrow$ as oxygen is placed below Ba, which in part neutralizes the Ti–O displacement induced polarization. One can see that the δ value is -0.087 Å for the top BaO ML (layer 2), while it is almost zero for the inner BaO ML (such as layer 4). The most interesting feature is that the δ values change from negative to positive values once $\varepsilon < -0.0475$, while it still keeps negative in the tension strain region. It is important to point out that the δ values are positive both in the TiO_2 and BaO layers for $\varepsilon < -0.0475$, indicating a significantly enhanced polarization in the viewpoint of displacement polarization theory.[11] Moreover, the structure distortion generally occurs on the top 1–2 unit cells of the surface in terms of the displacements of BaO and TiO_2 MLs, which is consistent with that of experimental results.[30]

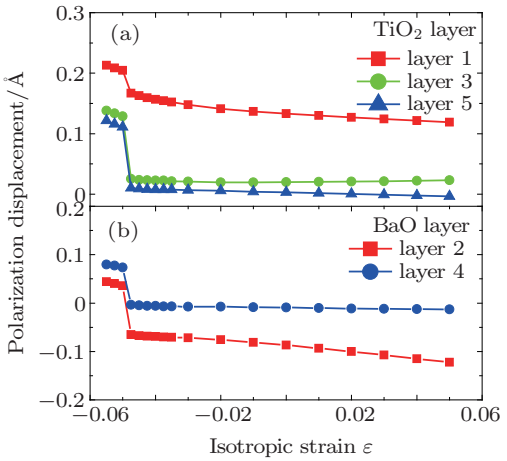


Fig. 2. (color online) Polarization displacements δ of (a) Ti–O layers and (b) Ba–O layers as a function of isotropic in-plane strain ε in TiO_2-terminated BTO (001) surface.

Next, the electronic structures under various strains are investigated by calculating their density of states (DOS). Figure 3 presents the total DOS data for several selected strains. A significant difference is found by comparing our results with the data for bulk BTO (~ 2.0 eV band gap).[11,27] The surface only has a band gap of ~ 0.78 eV at $\varepsilon = 0$, which is reasonable when comparing with a 0.8 eV band gap in a 4-unit cell BTO obtained using the full-potential linearized augmented plane-wave method[11] and a metallic state predicted by Fethner *et al.*[27] using the VASP method. It is worth noting that the band gap increases gradually with increasing tension train. However, an opposite trend is found when compressive strain increases until the band gap vanishes roughly at $\varepsilon = -0.0475$, where the dot circle shows an obvious in-gap state. Besides, the total DOS in the conduction and valence bands become more delocalized when increasing compressive strain.

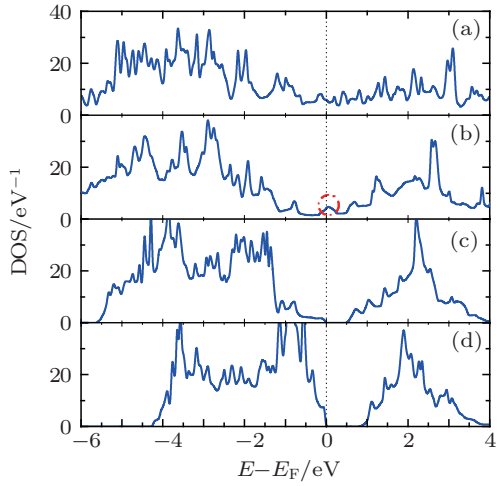


Fig. 3. (color online) Total density of states of the TiO_2-terminated BTO (001) surfaces for several selected epitaxial strains. (a) $\varepsilon = -0.05$, (b) $\varepsilon = -0.0475$, (c) $\varepsilon = -0.03$, (d) $\varepsilon = 0$.

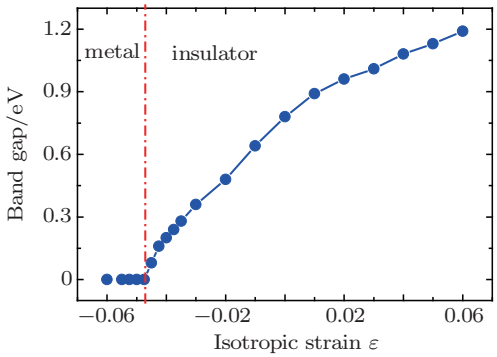


Fig. 4. (color online) Band gap as a function of isotropic strain ε for TiO_2-terminated BTO (001) surface.

A clear relationship between band gap and strain is shown in Fig. 4, where the band gap refers to the energy difference between the top of the valence band and the bottom of the conduction band of DOSs shown in Fig. 3. From Fig. 4, one can see clearly that the band gap becomes zero at $\varepsilon < -0.0475$, implying the occurrence of a metallic state. This result is consistent with that of calculated atom displacement. Similar results have been extensively reported.[15,16,31,32] Actually, the strain or stress has also played important roles in engineering properties in other materials, for example, strain-mediated electronic properties[32–34] and the mobility of charge carrier in semiconductors.[35]

To understand the inter-transition of the enhanced polarization and metallic state for this special TiO_2-terminated surface modulated by the compressive strain, we plot the partial DOS data for Ba 5p, O 2p, and Ti 3d orbitals at $\varepsilon = -0.045$, as shown in Fig. 5. It is clearly seen that the in-gap states are attributed to Ti, O, and Ba in order of importance. Compared with the total DOS shown in Fig. 3, the Ti 3d conduction band is shifted downward by ~ 0.16 eV into the band gap region, while the O 2p valence bands are shifted upward in energy by ~ 0.25 eV into the in-gap states. The present results are in good agreement with earlier data,[21] and the origin of conduction can be identified. The surface conductance of BTO single crystals in ultra-high vacuum below T_C was observed in experiment, and the reasons have been attributed as the occurrence of intrinsic surface electron–hole layer due to the surface rumpling or polar surface. Our results shown in Fig. 2 do present remarkable surface rumpling in case of highly compressive strain, which is at least qualitatively consistent with experimental observations.

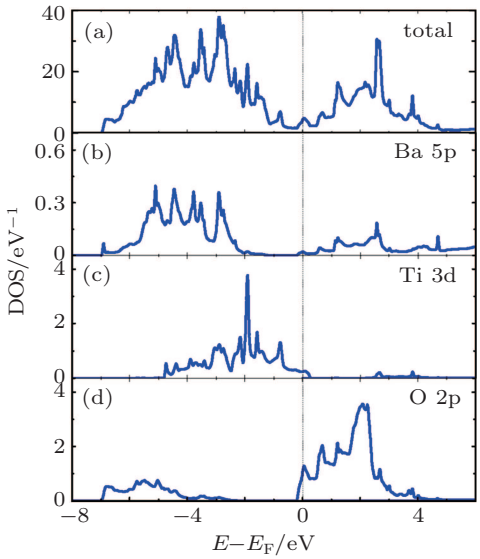


Fig. 5. (color online) (a) Total and partial density of states of (b) Ba 5p, (c) Ti 3d, and (d) O 2p orbitals on the BTO (001) surface at $\varepsilon = -0.0475$.

For a deeper view of the electronic structure, we also present the y–z plane projected charge density distributions along the [100] axis, as shown in Fig. 6, where the data for $\varepsilon = -0.0475$ and $\varepsilon = 0$ are plotted respectively, and the arrows indicate the polarization directions within each ML. It is observed that the charges between Ti (or Ba) and its nearest O ions do not have much hybridization at $\varepsilon = 0$, and only a weak hybridization between Ti in the layer 1 and O in the layer 2 is

identifiable as pointed out by the dot circle. This shows a sort of blockade for the charge transfer in the three directions. As a consequence, an insulator behavior is expected. However, for $\varepsilon = -0.0475$ on the y–z plane, the atoms are forced to move along the z axis. In addition to the induced polarization displacement, this leads to the in-plane hybridizations between Ti and its nearest O atoms, as shown by the dot circles, while the blockade is only identifiable along the z axis. Therefore, one is allowed to claim the charge redistribution and transfer on the top layer, making electrons delocalized and movable between the O 2p orbital and Ti 3d orbital. Furthermore, it is expected that the in-plane conductance should be better than the out-of-plane one along the z axis, which reasonably explains the anisotropic conduction on the surface of BTO single crystal.[27] In case of tension strain, the charge density distribution shows little difference from that at $\varepsilon = 0$, and only the conduction-band Ti 3d orbital and valence-band O 2p orbital become more localized.

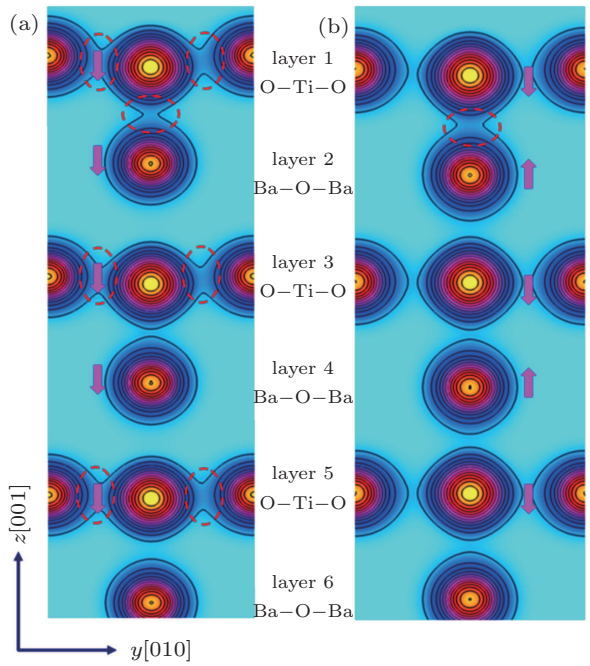


Fig. 6. (color online) The charge density contribution along [100] direction calculated for TiO_2-terminated BTO (001) surface and projected on the y–z plane for two cases: $\varepsilon = -0.0475$ (a), and $\varepsilon = 0$ (b). Dipole directions within each layer are labeled by the arrows. The contour set size is 0.01 e/Å^2.

4. Conclusion

In summary, we have carried out calculations of the electronic structure and charge distribution of Ti-terminated BTO (001) surface in response to the in-plane lattice strain by using first-principle methods. The results have predicted a strain-induced transition between insulating and metallic states near $\varepsilon = -0.0475$. The conductance mechanisms have been clarified as the strong hybridization of Ti 3d and O 2p orbitals, especially in x–y plane, which pushes the Ti 3d conduction band and O 2p valence band states to shift into the band gap. Our results indicate a promising way of engineering the electronic properties of ultra-thin BTO (001) films.

References

[1] Scott J F 2000 *Ferroelectric Memories* (Springer: Berlin) p. 247
[2] Park K I, Xu S, Liu Y, Hwang G T, Kang S J L, Wang Z L and Lee K J 2010 *Nano Lett.* **10** 4939
[3] Choi K J, Biegalski M, Li Y L, Sharan A, Schubert J, Uecker R, Reiche P, Chen Y B, Pan X Q, Gopalan V, Chen L Q, Schlom D G and Eom C B 2004 *Science* **5** 1005
[4] Lee H N, Christen H M, Chisholm M F, Rouleau C M and Lowndes D H 2005 *Nature* **433** 395
[5] Kreisel J, Weber M C, Dix N, Sanchez F, Thomas P A and Fontcuberta J 2012 *Adv. Funct. Mater.* **22** 5044
[6] Wen Z, Li C, Wu D, Li A D and Ming N B 2013 *Nat. Mater.* **12** 617
[7] Meyerheim H L, Klimenta F, Ernst A, Mohseni K, Ostanin S, Fechner M, Parihar S, Maznichenko I V, Mertig I and Kirschner J 2011 *Phys. Rev. Lett.* **106** 087203
[8] Plodinec M, Santic A, Zavasnik J, Ceh M and Gajovic A 2014 *Appl. Phys. Lett.* **105** 152101
[9] Li C J, Huang L S, Li T, Lu W M, Qiu X P, Huang Z, Liu Z Q, Zeng S W, Guo R, Zhao Y L, Zeng K Y, Coey J M D, Chen J S, Ariando and Venkatesan T 2015 *Nano Lett.* **15** 2568
[10] Chen J P, Luo Y, Ou X, Yuan G L, Wang Y P, Yang Y, Yin J and Liu Z G 2013 *J. Appl. Phys.* **113** 204105
[11] Cai M Q, Du Y and Huang B Y 2011 *Appl. Phys. Lett.* **98** 102907
[12] Stengel M, Vanderbilt D and Spaldin N A 2009 *Nat. Mater.* **8** 392
[13] Lu H, Liu X, Burton J D, Bark C W, Wang Y, Zhang Y, Kim D J, Stamm A, Lukashev P, Felker D A, Folkman C M, Gao P, Rzchowski M S, Pan X Q, Eom C B, Tsymbal E Y and Gruverman A 2012 *Adv. Mater.* **24** 1209
[14] Damodaran A R, Breckenfeld E, Chen Z H, Lee S K and Martin L W 2014 *Adv. Mater.* **26** 6341
[15] Haeni J H, Irvin P, Chang W, Uecker R, Reiche P, Li Y L, Choudhury S, Tian W, Hawley M E, Craigo B, Tagantsev A K, Pan X Q, Streiffer S K, Chen L Q, Kirchoefer S W, Levy J and Schlom D G 2004 *Nature* **430** 758
[16] Lee D, Lu H, Gu Y, Choi S Y, Li S D, Ryu S, Paude T R, Song K, Mikheev E, Lee S, Stemmer S, Tenne D A, Oh S H, Tsymba E Y, Wu X, Chen L Q, Gruverman A and Eom C B 2015 *Science* **349** 1314
[17] Paul J, Nishimatsu T, Kawazoe Y and Waghmare U V 2007 *Phys. Rev. Lett.* **99** 077601
[18] Schilling A, Prosandeev S, McQuaid R G P, Bellaiche L, Scott J F and Gregg J M 2011 *Phys. Rev. B* **84** 064110
[19] Hirai K, Kan D, Ichikawa N, Mibu K, Yoda Y, Andreeva M and Shimakawa Y 2015 *Sci. Rep.* **5** 7894
[20] Dieguez O, Rabe K M and Vanderbilt D 2005 *Phys. Rev. B* **72** 144101
[21] Yang Q, Cao J X, Ma Y, Zhou Y C, Lou X J and Yang J 2013 *J. Appl. Phys.* **114** 034109
[22] Yang Q, Cao J X, Zhou Y C, Zhang Y, Ma Y and Lou X J 2013 *Appl. Phys. Lett.* **103** 142911
[23] Tenne D A, Turner P, Schmidt J D, Biegalski M, Li Y L, Chen L Q, Soukiassian A, Trolier-McKinstry S, Schlom D G, Xi X X, Fong D D, Fuoss P H, Eastman J A, Stephenson G B, Thompson C and Streiffer S K 2009 *Phys. Rev. Lett.* **103** 177601
[24] Shin J, Nascimento V B, Borisevich A Y, Plummer E W, Kalinin S V and Baddorf A P 2008 *Phys. Rev. B* **77** 245437
[25] Meyerheim H L, Ernst A, Mohseni K, Maznichenko I V, Ostanin S, Klimenta F, Jedrecy N, Feng W, Mertig I, Felici R and Kirschner J 2012 *Phys. Rev. Lett.* **108** 215502
[26] Iles N, Driss K K, Kellou A and Aubert P 2014 *Comp. Mater. Sci.* **87** 123
[27] Fechner M, Ostanin S and Mertig I 2008 *Phys. Rev. B* **77** 094112
[28] Kresse G and Furthmuller J 1996 *Phys. Rev. B* **54** 11169
[29] Gajdos M, Hummer K, Kresse G, Furthmüller J and Bechstedt F 2006 *Phys. Rev. B* **73** 045112
[30] Li Y L, Yu R, Shi T, Liao Z Y, Song D S, Zhou H H, Cheng Z Y and Zhu J 2015 *J. Phys.: Condens. Matter* **27** 095901
[31] Tian X B, Yang X H and Cao W Z 2013 *J. Eelectron. Mater.* **42** 2504
[32] Ni L H, Liu Y, Ren Z H, Song C L and Han G R 2011 *Chin. Phys. B* **20** 106102
[33] Rodin A S, Carvalho A and Castro Neto A H 2014 *Phys. Rev. Lett.* **112** 176801
[34] Torre A L, Botello-Mendez A, Baaziz W, Charlier J C and Banhart F 2015 *Nat. Commun.* **6** 6636
[35] Chen Z P, He J J, Zhou P, Na J and Sun L Z 2015 *Comp. Mater. Sci.* **110** 102